

Beams with bonded-on steel plates : design for shear

Autor(en): **Jansze, Wim / Uijl, Joop A. den / Walraven, Joost C.**

Objektyp: **Article**

Zeitschrift: **IABSE reports = Rapports AIPC = IVBH Berichte**

Band (Jahr): **999 (1997)**

PDF erstellt am: **29.06.2024**

Persistenter Link: <https://doi.org/10.5169/seals-1048>

Nutzungsbedingungen

Die ETH-Bibliothek ist Anbieterin der digitalisierten Zeitschriften. Sie besitzt keine Urheberrechte an den Inhalten der Zeitschriften. Die Rechte liegen in der Regel bei den Herausgebern.

Die auf der Plattform e-periodica veröffentlichten Dokumente stehen für nicht-kommerzielle Zwecke in Lehre und Forschung sowie für die private Nutzung frei zur Verfügung. Einzelne Dateien oder Ausdrucke aus diesem Angebot können zusammen mit diesen Nutzungsbedingungen und den korrekten Herkunftsbezeichnungen weitergegeben werden.

Das Veröffentlichen von Bildern in Print- und Online-Publikationen ist nur mit vorheriger Genehmigung der Rechteinhaber erlaubt. Die systematische Speicherung von Teilen des elektronischen Angebots auf anderen Servern bedarf ebenfalls des schriftlichen Einverständnisses der Rechteinhaber.

Haftungsausschluss

Alle Angaben erfolgen ohne Gewähr für Vollständigkeit oder Richtigkeit. Es wird keine Haftung übernommen für Schäden durch die Verwendung von Informationen aus diesem Online-Angebot oder durch das Fehlen von Informationen. Dies gilt auch für Inhalte Dritter, die über dieses Angebot zugänglich sind.

Beams with Bonded-on Steel Plates: Design for Shear

Wim JANSZE

Assistant Researcher
Delft University of Technology
Delft, The Netherlands

Wim Jansze, born in 1966, graduated in civil engineering from the TUD in 1993. Till May 1997 he worked as assistant researcher at the Stevin Laboratory on structural members strengthened with externally bonded steel plates.

Joop A. DEN UIJL

Senior Researcher
Delft University of Technology
Delft, The Netherlands

Joop den Uijl, born in 1947, obtained his civil engineering degree in 1972 at TUD. In 1972 he joined the Stevin Laboratory for research. Currently, he works as a senior researcher on bond-related topics.

Joost C. WALRAVEN

Professor
Delft University of Technology
Delft, The Netherlands

Joost Walraven, born in 1947, received his degree in civil engineering in 1972 at TUD, in 1980 his doctor degree by research on aggregate interlock. Since 1989 he is professor of the Concrete Structures Group.

Summary

A fictitious shear span is formulated for members without web reinforcement which are partially strengthened with externally bonded steel plates. An analytical expression for this fictitious shear span is derived based on tests and simulations. Then, by using MC90, the resistance by plate-end shear for partially plated members is calculated. In addition, for fully plated members the flexural-shear resistance is calculated with Rafla's formulation. Kani's shear valley for plate-end shear indicates that this type of behaviour dominates flexural shear.

1. Introduction

In practice, strengthening of RC members with externally bonded steel plates has mainly been applied in order to improve their flexural capacity. But how does the additionally bonded flexural reinforcement influence the shear resistance of the member? Oehlers [1992] investigated the shear resistance of members without web reinforcement by varying the "unplated length of the shear span." However, due to the scatter of test results the influence was not clearly shown.

Formulations for the mean value of the ultimate shear stress τ_{um} for conventionally RC members without web reinforcement were given by Rafla (Eq. (1)) and MC90 (Eq. (2)). After statistical analyses it emerged that for $C_{m,Rafla} = 0.85$ and $C_{m,MC90} = 0.18$ good agreement with test results on the ultimate nominal shear stress is obtained (Jansze [1997]). Then, the shear load V_{um} is simply calculated by multiplying τ_{um} with bd . These formulations and a formulated fictitious shear span for plate-end shear form the basis for a design method for plated members loaded in shear.

2. Analyses of variables influencing the shear capacity

2.1. Framework of the research study

At the Delft University of Technology a research study was conducted in which the influence of the unplated length L , the plate reinforcement ratio ρ_p (by varying plate width and thickness) and the shear span a were investigated (Jansze [1997]). The test set-up provided a shear span of 800 mm. The specimens were 100×200 mm² in cross section and contained two longitudinal 8 mm diameter ribbed bars at an effective depth of 170 mm. No web reinforcement was applied.

Rafla Eq. (1)	CEB-FIP MC90 Eq. (2)
$\tau_{um} = C_{m,Rafla} \alpha_u \sqrt{f_{cm}} \sqrt[3]{\rho_0} d^{-0.25}$	$\tau_{um} = C_{m,CEB} \sqrt[3]{3 \frac{d}{a} (1 + \sqrt{\frac{200}{d}})^3 \rho_0 f_{cm}}$
$\alpha_u = 6.0 - 2.2 \frac{a}{d}$ for $1.0 < \frac{a}{d} < 2.0$	$V_{um} = \tau_{um} bd$ in which: ρ_0 = reinforcement ratio ($=100A_s/bd$) f_{cm} = mean compressive cylinder strength d = effective depth a = shear span
$\alpha_u = 0.795 + 0.293(3.5 - \frac{a}{d})^{2.5}$ for $2.0 < \frac{a}{d} < 3.5$	
$\alpha_u = 0.90 - 0.03 \frac{a}{d}$ for $3.5 < \frac{a}{d}$	

2.2. Experimental observations and numerical simulations on shear

Tests and numerical simulations showed a good agreement (Fig. 1). In the case of a fully plated specimen (L0), flexural-shear failure occurred in the shear span. The ultimate shear load was correctly calculated by Rafla's equation. However, when the shear span was only partially plated (L50, L100, L200), a large crack was initiated at the plate end in the unstrengthened part of the shear span. This crack developed into a shear crack at the onset of the ultimate load. Thus, failure is governed by plate-end shear. The FEM-simulations were carried out with DIANA. For concrete cracking the smeared crack model with bilinear tension softening was adopted.

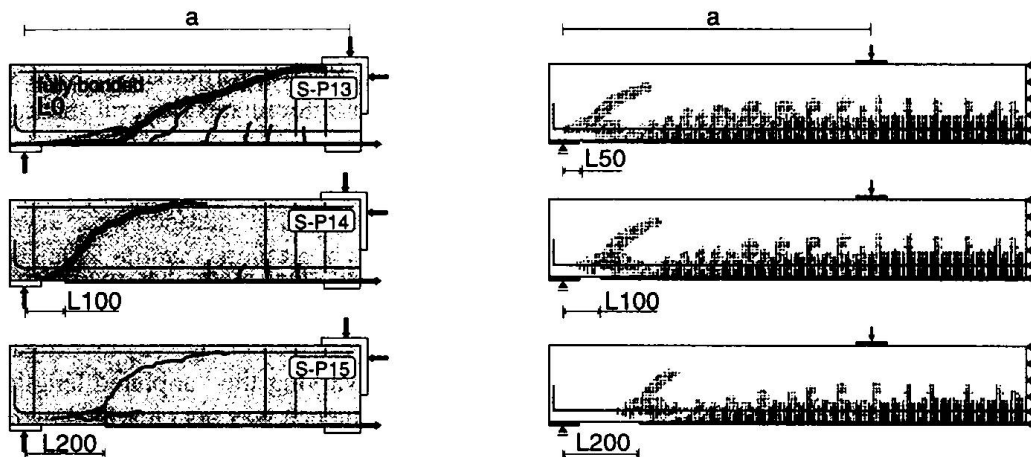


Fig. 1 Crack pattern after testing (left: L0, L100 and L200) and numerically calculated crack pattern at ultimate load (right: L50, L100, L200) of strengthened member with $5 \times 100 \text{ mm}^2$ plate

2.3. Qualification of variables

When the results obtained from the experiments and the numerical simulations are graphically represented, the following conclusions with respect to the variables can be drawn:

- The unplated length L mainly governs the magnitude of the ultimate shear load, see Fig. 2. From about unplated lengths larger than 300 mm a combined shear-flexural peeling occurs;
- The shear span a has no influence on the ultimate shear load if $a > L + d$, see Fig. 3;
- The amount of plate reinforcement ρ_p (by varying cross sectional area) has little effect on the ultimate load by plate-end shear compared with flexural shear (L0), see Fig. 4.

Flexural shear can be described with conventional formulas in contrast to plate-end shear. For the derivation of an analytical expression to describe the shear resistance by plate-end shear, only the influence of the unplated length L is taken into account.

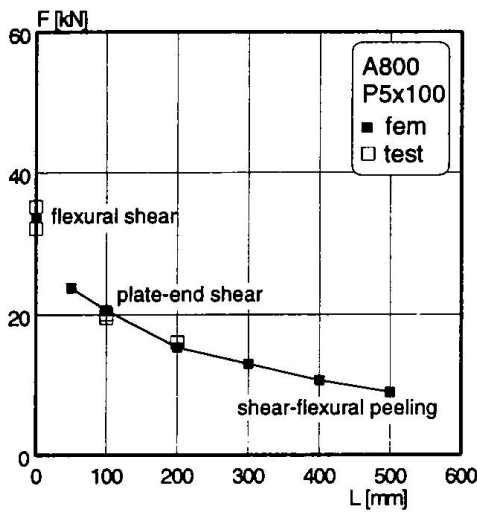


Fig. 2 Influence of unbonded length L on shear capacity

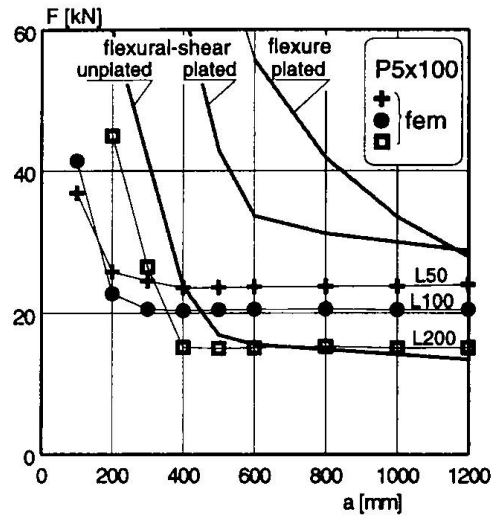


Fig. 3 Influence of shear span a on shear capacity as a function of L

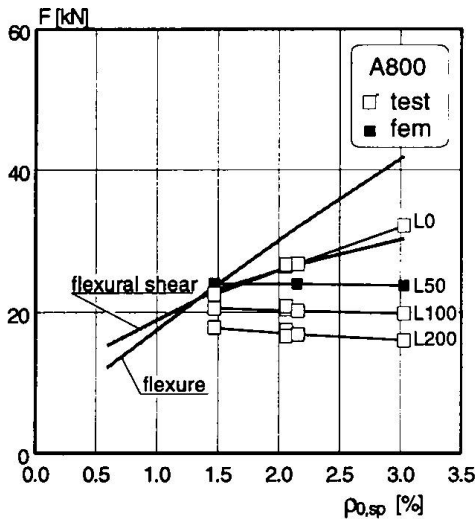


Fig. 4 Influence of reinforcement ratio $\rho_{0,sp}$ on shear capacity as function of L

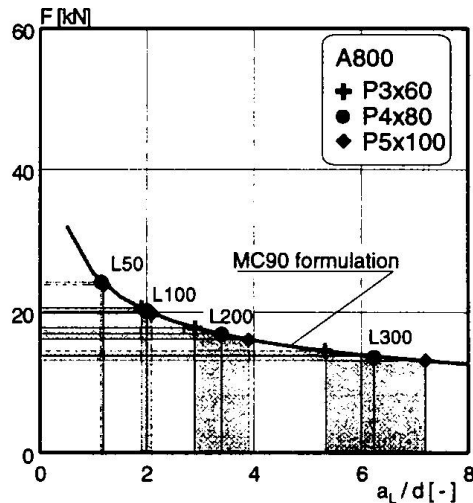


Fig. 5 Fictitious a_l / d according to tests and calculations on basis of MC90

3. Formulation for predicting the plate-end shear capacity

3.1. Additional parameter: fictitious shear span a_l

The plate-end-shear crack prevents the partially plated specimen to take full advantage of arch action due to intersection of the compressive-force path. Thus, only the contribution of beam action can be accounted for. When the ultimate shear loads of the partially plated members are compared with the shear resistance formulation of MC90 - which insufficiently takes full arch action into account compared to Rafla's equation (see Jansze [1997]) - a fictitious shear-span-to-depth ratio can be defined, see Fig. 5. Because the effective depth d_e of the unplated part is constant, a fictitious shear span a_l can be deduced, see Table 1. From this Table it follows that the fictitious shear span a_l increases with increasing unplated length L . At the same time, the

fictitious shear span also increases with increasing cross sectional area of the steel, however, this will be neglected. Note that the real shear span a of the member is 800 mm.

Table 1 Fictitious shear span a_l deduced from ultimate plate-end-shear loads and MC90

Member	L50		L100		L200		L300	
	a_l/d [-]	a_l [mm]	a_l/d [-]	a_l [mm]	a_l/d [-]	a_l [mm]	a_l/d [-]	a_l [mm]
P3x60	1.1	187	1.9	325	2.9	495	5.3	901
P4x80	1.15	195	2.0	340	3.4	580	6.2	1054
P5x100	1.2	205	2.1	355	3.9	665	7.2	1225

3.2. Modelling analogy

By introducing the fictitious shear span an analogy was found with Kim & White [1991]. There, an analytical expression was developed for predicting the location of the critical shear crack on the basis of ρ , a and d . Because limited data was available on the exact location of the critical crack position a_c , a statistical analysis resulted in Eq. (3), see Fig. 6 (left) (note: $\rho = \rho_s = A_s/bd$).

If RC members are partially strengthened by means of externally bonded steel plates, it was demonstrated that a plate-end-shear crack is forced to occur in the unplated part of the shear span. Hence, the position of the unbonded length L is fixed and equals to location of the critical shear crack a_c of Kim & White. Accordingly, the fictitious shear span a_l is analogous to the shear span a belonging to a_c . Then, Eq. (3) can be interpreted as Eq. (4), see also Fig. 6 (right).

$$a_c = 3.3 \left[\frac{\rho \left(\frac{d}{a} \right)^2}{(1-\sqrt{\rho})^2} \right]^{1/3} a \quad \text{Eq.(3)} \quad \xRightarrow{\text{modelling analogy}} \quad L = 3.3 \left[\frac{\rho_s \left(\frac{d_s}{a_l} \right)^2}{(1-\sqrt{\rho_s})^2} \right]^{1/3} a_l \quad \text{Eq.(4)}$$

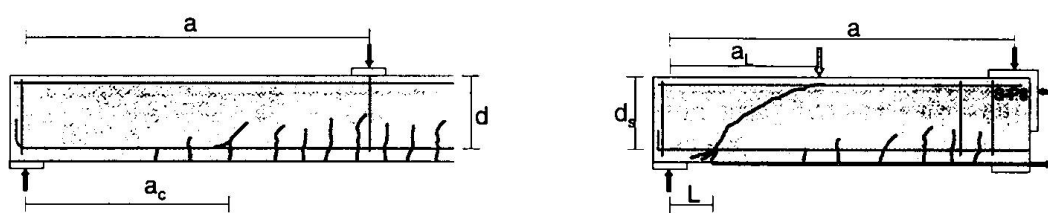


Fig. 6 Location a_c of governing flexural-shear crack according to Kim & White [1991] Modelling analogy with fictitious shear span a_l and unplated length L for partially plated member according to Jansze [1997]; plate-end-shear crack is analogous to flexural-shear crack

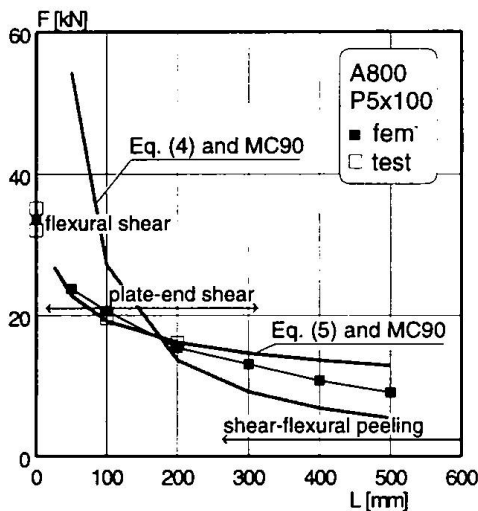
3.3. Verification and formulation of shear resistance by fictitious shear span

The fictitious shear span a_l as expressed by Eq. (4) is used to compute the shear resistance on the basis of MC90. Essential is that in this formulation the unstrengthened part is considered, so the effective depth of the internal reinforcement d_s and the internal reinforcement ratio ρ_s have to be considered. In Fig. 7 the computed shear resistance is compared with the experimental and numerically simulated results. It can be seen that the constant 3.3 of Kim & White overestimates the plate-end-shear load. However, analyses show that by replacing the constant 3.3 in Eq. (4) by the fictitious-shear-span-to-depth ratio a_l/d_s , good agreement is obtained between the plate-end-shear loads based on the fictitious shear span and the experimental and numerical results,

see Fig. 7. Thus, by substituting constant 3.3, Eq. (4) can be rewritten into Eq. (5) that explicitly expresses the fictitious shear span a_L :

$$a_L = \sqrt[4]{\frac{(1 - \sqrt{\rho_s})^2}{\rho_s} d_s L^3} \tag{Eq. (5)}$$

For L50, L100, L200 and L300 a fictitious shear span of respectively 235, 395, 665 and 900 mm is calculated. These values are very satisfactory when compared to Table 1. Then, when the fictitious shear span calculated by Eq. (5) is subsequently used to calculate shear according to MC90, the plate-end-shear loads are in good agreement with the tests and simulations. When Eq. (5) is used to calculate the shear resistance of various concrete member geometry's as listed in Table 2, it is concluded that the analytical expression in combination with MC90 is definitely capable of calculating the plate-end-shear load of partially strengthened members. This method is applicable for $a > L+d$. Furthermore, Jansze [1997] shows that this method is also applicable to determine a lower bound for shear peeling loads, and not applicable for shear-flexural peeling.



Tests	series	series
Jansze [1997]	S-W	S-H
A_c [mm ²]	200x200	100x400
ρ_{ad} [%]	0.59	0.662
P [mm ²]	5x100	5x100
L [mm]	100	200
a [mm]	800	1600
a_L [mm]	395	795
V_{cap} [kN]	35.9 / 36.5	38.1 / 40.6
V_{un} [kN]	35.8 / 36.9	40.3 / 34.4
V_{un} [kN]	37.7	36.5

Fig. 7 Shear resistance of tests, simulations and according to model

Table 2 Shear resistance of additional tests according to fictitious shear span and MC90

4. Shear - Flexure interaction represented by Kani's shear valley

4.1. Input parameters for a case study

A case study is carried out in which the shear-flexure interaction is analysed by constructing Kani's shear valley for fully and partially plated members. For various shear-span-to-depth and reinforcement ratios the ultimate shear moment over ultimate flexural moment is calculated. A maximum value of $M_{vcu} / M_{flex} = 1$ is adopted to indicate flexural failure. The case study is based on a member 100x200 mm² in cross section and the amount of external plate reinforcement is assumed to be equal to the amount of internal bars ($\rho_s = \rho_p$). Flexural failure is calculated by adopting yield stresses of 600 N/mm² and 285 N/mm² for the bars and plate, respectively. The mean compressive cylinder strength is 36 N/mm². It must be stressed that at the axes the total amount of reinforcement is based on the reinforcement ratio in the constant moment region ($\rho_s + \rho_p$) and furthermore that the real shear span a is plotted in the graph for a/d .

4.2. Flexural capacity versus flexural-shear and plate-end-shear resistance

Both flexural shear for fully plated members (L0) and plate-end shear for partially plated members (in this case study $L = 100$ and 200 mm) are graphically represented by Kani's shear valley in Fig. 8. It is clearly seen that for plate-end shear Kani's shear valley has much more depth than for flexural-shear failure. Particularly for shear-span-to-depth ratio's $a/d < 4$ or 5 plate-end shear dominates flexural shear. For shear spans smaller than approximately $a < L+d$ an arch can be formed between the load and the support because the plate-end-shear crack does not intersect the compressive-load path. Thus, a plateau is visible as in the original shear valley. The valley of the L200 member has less depth than that of the L100 member, see also Fig. 3. The L100 and L200 graphs further indicate that with increasing unplated length plate-end-shear also governs failure for larger a/d -values. The graphs clearly indicate that one should be careful with strengthening short deep beams. The reduction of the bearing capacity by plate-end shear may be considerable, specially for small a/d -values.

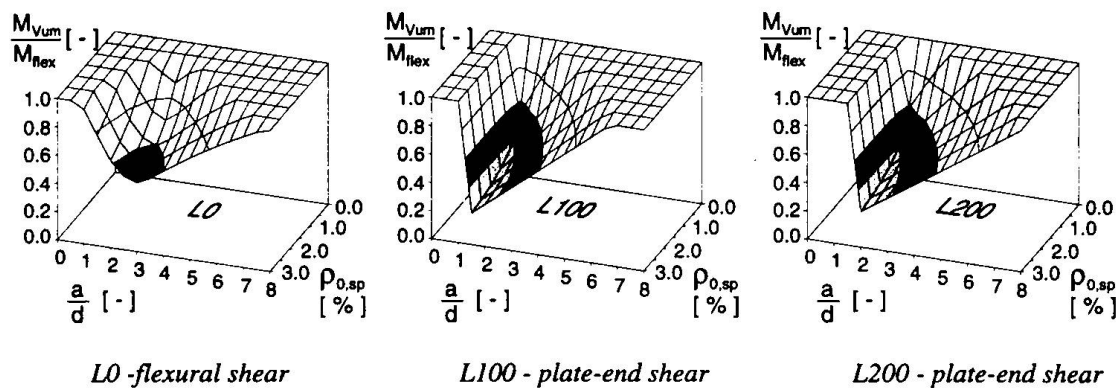


Fig. 8 Kani's shear valley for fully plated members and calculated Kani's shear valley for partially plated members with external steel plate stopped 100 and 200 mm short of the support

5. Conclusions

The fictitious-shear-span-to-depth ratio is successfully used in combination with the MC90 formulation on shear resistance to calculate the ultimate shear load for plate-end shear. Basically, the mechanism of plate-end shear is analogous to that of flexural shear, however, the ultimate shear loads differ significantly. Compared to the flexural capacity, up to about $a/d < 4$ or 5 , failure by plate-end shear dominates failure by flexural shear. It is therefore advised to bond the steel plate as close as possible to the support to increase not only the flexural capacity, but also the shear resistance of the strengthened member.

Oehlers, D.J. [1992]. Reinforced concrete beams with plates glued to their soffits. *Journal of Structural Engineering*, Vol. 118, No. 8, August 1992, pp. 2023-2038.

Kim, W. and White, R.N. [1991]. Initiation of Shear Cracking in Reinforced Concrete Beams with No Web Reinforcement, *ACI Structural Journal*, V.88, No.3, May-June 1991, pp 301-308.

Jansze, W. [1997]. Strengthening with Externally Bonded Steel Plates: Design for Beam Shear and Plate Anchorage, *Dissertation*, Delft University of Technology, To be published in 1997.